Accuracy of Joint Time-Based and Carrier-Phase Positioning in 5G Networks under Correlated Measurement Errors

Nahidul Islam*, Mohammad Razzaghpour*†, Marwan Hammouda*, Carsten Bockelmann*, and Armin Dekorsy*†
* Dept. of Communications Engineering, University of Bremen, Germany
† Gauss-Olbers Space Technology Transfer Center, University of Bremen, Germany
Emails: nahidul@uni-bremen.de, {razzaghpour, hammouda, bockelmann, dekorsy}@ant.uni-bremen.de

***Abstract*—High-accuracy positioning is critical for emerging applications such as autonomous driving, industrial automation, augmented reality, and smart cities. 3GPP Release 18 introduced carrier-phase (CP) positioning for 5G as a method that offers superior accuracy compared to conventional time-based methods such as time of arrival (ToA). However, CP-based positioning requires resolving the integer phase ambiguity, which refers to the unknown number of full-wavelength cycles completed during signal propagation. Joint processing of ToA and CP can mitigate this integer ambiguity by narrowing down the search space of possible integers, particularly for short wavelengths. This paper investigates the performance of a positioning method that integrates ToA and CP measurements. As a main contribution, the analysis explicitly accounts for the error correlation between ToA and CP measurements. Furthermore, the study analyzes the impact of key 5G system parameters on positioning accuracy using this correlation-aware joint method in both factory and urban environments, where many 5G positioning applications are expected to emerge. The results highlight that exploiting this correlation can further improve positioning performance by approximately 7 percent. Moreover, the findings of this study provide insight into how 5G system parameters can be tuned to improve positioning accuracy and, under favorable conditions, achieve centimeter-level accuracy.**

***Index Terms*—Carrier phase positioning, time of arrival, correlated error, 5G new radio (NR), 3GPP Release 18.**

I. Introduction

As wireless technology evolves from 5G to 5G-Advanced and eventually to 6G, positioning has emerged as a key capability [1]. By leveraging wider bandwidths, higher carrier frequencies, multiple-input multiple-output (MIMO), and dense network infrastructure, 5G can achieve positioning accuracy that was previously unattainable in earlier generations of cellular networks. This improved accuracy is essential for enabling a wide range of emerging applications, from autonomous driving and industrial robotics to augmented reality and smart cities.

Conventional radio positioning techniques determine the location of a mobile terminal (MT) through time of arrival (ToA), received signal strength (RSS), and angle of arrival (AoA) measurements. The accuracy of these methods is limited by factors such as measurement precision and resolution, signal processing techniques, and the radio propagation environment. In 5G, traditional time-based methods can achieve sub-meter accuracy under favorable conditions, e.g., when the maximum available bandwidth is used [2].

To further improve positioning accuracy, 3GPP Release 18 has recently introduced carrier phase (CP) positioning techniques for 5G [3], [4]. This idea builds on the well-established use of CP-based methods in global navigation satellite system (GNSS), such as real-time kinematic (RTK) and precise point positioning (PPP), which can achieve centimeter-level accuracy when GNSS satellite signals are available.

Generally, CP-based methods suffer from the so-called integer phase ambiguity, defined as the unknown number of whole carrier wavelengths traversed by the radio wave during propagation from transmitter to receiver, since the phase repeats itself every complete cycle, i.e., every 2π. The main challenge in resolving this phase ambiguity is the large search space of possible integers, especially for mmWave frequencies.

In [5], integer ambiguity is resolved using a multi-frequency carrier method. Alternatively, when multi-frequency carrier-phase measurements are unavailable, the search space for the integer ambiguities can be reduced by combining time-based measurements with a CP-based approach [6]. Regarding techniques that integrate ToA and CP measurements, [1] employs analytical tools such as the Cramér-Rao lower bound (CRLB) to determine their theoretical positioning accuracy limits, thereby providing a benchmark for evaluating practical implementations. However, it does not consider the correlations between the measurement errors of ToA and CP, which may exist in practical setups. This correlation arises because ToA and CP are derived from the same received signal and are affected by common error sources, such as multipath effects, clock synchronization mismatch between the base stations (BSs) and the MT, and thermal noise. However, the impact of correlated ToA and CP measurement errors has received limited attention in the existing literature.

In this paper, we propose and evaluate a joint positioning

This work is supported by the Federal Ministry of Economic Affairs and Climate Action of Germany on the basis of a decision by the German Bundestag.

method that integrates ToA and CP measurements while explicitly accounting for correlated measurement errors. Furthermore, using this correlation-aware joint method, we investigate the impact of key 5G parameters on positioning accuracy, including carrier frequency, bandwidth, transmit power, antenna configurations, and the number of involved BSs.

The rest of the paper is organized as follows: Section II introduces the correlation-aware joint positioning method, Section III outlines the simulation setup, Section IV presents and discusses the results, and Section V concludes the paper.

II. Correlation-Aware Joint Positioning Method

A. System and Received Signal Model

Consider a 5G network, as shown in Fig. 1, comprising an MT located at an unknown position $\mathbf{x} = [x\ y]^\mathsf{T}$ and $N \geq 3$ BSs with known positions $\mathbf{x}_i = [x_i\ y_i]^\mathsf{T}$. This study considers downlink positioning only. Let $s(t)$ denote the transmitted downlink positioning reference signal (PRS) from the i-th BS. Assuming a line-of-sight wireless channel, the baseband-equivalent received signal at the MT from the i-th BS is given by

$$y_i(t) = a_i e^{j\phi_i} s(t - \tau_i) + w_i(t), \tag{1}$$

where a_i is the attenuation, τ_i is the propagation delay (ToA), ϕ_i is the carrier phase, and $w_i(t)$ is the zero-mean additive white Gaussian noise (AWGN) with variance $\sigma_w^2 = N_0 B$, where N_0 is the power spectral density (PSD) and B is the bandwidth. The attenuation a_i captures the combined effects of path loss and antenna gains, as follows

$$a_i = \sqrt{P_{\mathrm{BS}_i} G_{\mathrm{BS}_i} G_{\mathrm{MT}} \left(\frac{\lambda}{4\pi d_0}\right)^2 \left(\frac{d_0}{d_i}\right)^\gamma}, \tag{2}$$

where P_{BS_i} is the transmit power of BS, G_{BS_i} and G_{MT} are antenna gains of BS and MT respectively, λ is the carrier wavelength, γ is the path loss exponent, d_0 is the reference distance, and $d_i = \|\mathbf{x} - \mathbf{x}_i\|_2$ is the distance between the MT and the i-th BS. The delay and the phase are geometrically related by

$$\tau_i = \frac{d_i}{c} \quad \text{and} \quad \phi_i = \frac{2\pi d_i}{\lambda}. \tag{3}$$

B. Joint Observation Model

From the received signal, ToA- and CP-based range measurements are obtained as

$$r_{\tau_i} = c\hat{\tau}_i = d_i + n_{\tau_i}, \tag{4}$$

$$r_{\phi_i} = \hat{z}_i \lambda + \frac{\lambda}{2\pi}\hat{\phi}_i = d_i + n_{\phi_i}, \tag{5}$$

where n_{τ_i} and n_{ϕ_i} are assumed to be zero-mean Gaussian measurement errors, considering perfectly synchronized BSs and negligible calibration offsets. The integer phase ambiguity estimate $\hat{z}_i$ is obtained using the traditional least-squares ambiguity decorrelation adjustment (LAMBDA) algorithm [7] after calculating the initial estimate by

$$\hat{z}_i^{\mathrm{init}} = \left\lfloor \frac{c\hat{\tau}_i}{\lambda} \right\rfloor. \tag{6}$$

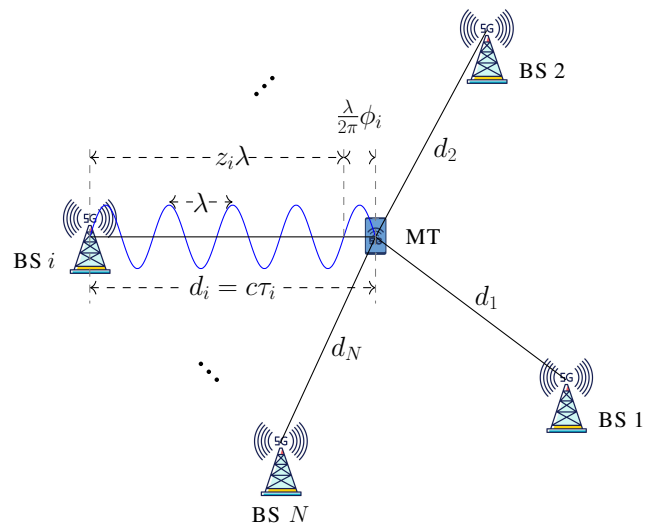

Fig. 1: ToA- and CP-based positioning measurements in 5G networks.

The standard deviations of n_{τ_i} and n_{ϕ_i} are given by [8]–[10]

$$\sigma_{\tau_i} \propto \frac{1}{B\sqrt{\mathrm{SNR}_i}}, \quad \sigma_{\phi_i} \propto \frac{1}{f_c\sqrt{\mathrm{SNR}_i}}, \tag{7}$$

respectively, where SNR_i is the signal-to-noise ratio (SNR) and f_c is the carrier frequency. Stacking observations from all N BSs, the joint observation model can be expressed as

$$\mathbf{r} = \boldsymbol{\mu}(\mathbf{x}) + \mathbf{n}, \tag{8}$$

where $\mathbf{r} = \left[\mathbf{r}_\tau^\mathsf{T}\ \mathbf{r}_\phi^\mathsf{T}\right]^\mathsf{T} \in \mathbb{R}^{2N}$ and $\mathbf{n} = \left[\mathbf{n}_\tau^\mathsf{T}\ \mathbf{n}_\phi^\mathsf{T}\right]^\mathsf{T} \in \mathbb{R}^{2N}$. The mean vector $\boldsymbol{\mu}(\mathbf{x})$ contains the true geometric distances between the MT and the BSs.

C. Proposed Error Correlation Model

We propose an error correlation model to explicitly account for the statistical dependence between ToA and CP measurement errors. To this end, the covariance matrix of the error vector $\mathbf{n}$ includes non-zero cross-covariance terms and is given by

$$\mathbf{C} = \begin{bmatrix} \mathbf{R}_\tau & \mathbf{R}_{\tau\phi} \\ \mathbf{R}_{\tau\phi}^\mathsf{T} & \mathbf{R}_\phi \end{bmatrix} \in \mathbb{R}^{2N\times 2N}. \tag{9}$$

Since the measurement errors are assumed to be uncorrelated across different BSs, the covariance matrices $\mathbf{R}_\tau$ and $\mathbf{R}_\phi$ can be written as

$$\mathbf{R}_\tau = \mathrm{diag}(\sigma_{\tau_1}^2, \ldots, \sigma_{\tau_N}^2) \in \mathbb{R}^{N\times N} \tag{10}$$

and

$$\mathbf{R}_\phi = \mathrm{diag}(\sigma_{\phi_1}^2, \ldots, \sigma_{\phi_N}^2) \in \mathbb{R}^{N\times N}. \tag{11}$$

As expressed in (7), the individual error variances depend on the bandwidth, carrier frequency, and the received SNR. The cross-covariance matrix is given by

$$\mathbf{R}_{\tau\phi} = \mathrm{diag}(\rho_{\tau_1\phi_1}\sigma_{\tau_1}\sigma_{\phi_1}, \ldots, \rho_{\tau_N\phi_N}\sigma_{\tau_N}\sigma_{\phi_N}) \in \mathbb{R}^{N\times N}, \tag{12}$$

where $\rho_{\tau_i \phi_i}$ is the correlation coefficient between ToA and CP measurement errors for the i-th BS, with $|\rho_{\tau_i \phi_i}| < 1$. This formulation incorporates error correlations through non-zero cross-covariance terms, thereby enabling the estimator to exploit the resulting information gains.

D. Position Estimation Model

The conditional probability density function (PDF) of $\mathbf{r}$ given $\mathbf{x}$ is expressed as

$$p(\mathbf{r} \mid \mathbf{x}) = \frac{1}{(2\pi)^N \sqrt{|\mathbf{C}|}} \exp\left(-\frac{1}{2}\left(\mathbf{r} - \boldsymbol{\mu}(\mathbf{x})\right)^{\mathsf{T}} \mathbf{C}^{-1} \left(\mathbf{r} - \boldsymbol{\mu}(\mathbf{x})\right)\right), \tag{13}$$

where $|\mathbf{C}|$ denotes the determinant of the covariance matrix of the error vector $\mathbf{n}$. Since the measurement errors are assumed to be Gaussian, the estimate of the MT position can be obtained using the maximum likelihood (ML) estimator by maximizing the PDF, i.e.,

$$\hat{\mathbf{x}} = \arg\max_{\mathbf{x}} p(\mathbf{r} \mid \mathbf{x}), \tag{14}$$

which is equivalent to a nonlinear weighted least-squares (WLS) problem given by

$$\hat{\mathbf{x}} = \arg\min_{\mathbf{x}} \left(\mathbf{r} - \boldsymbol{\mu}(\mathbf{x})\right)^{\mathsf{T}} \mathbf{C}^{-1} \left(\mathbf{r} - \boldsymbol{\mu}(\mathbf{x})\right). \tag{15}$$

The resulting optimization problem is nonlinear and can be solved using iterative optimization techniques, such as the Gauss–Newton method. The computational complexity scales with the number of BSs and is dominated by the inversion of the covariance matrix.

III. Simulation Setup

A. Path Loss Parameters

To ensure realistic deployment conditions, we choose the path-loss model parameters according to the 3GPP specifications for indoor factory (InF) and urban macro (UMa) deployments [11]–[13]. Assuming unity antenna gains, i.e., 0 dBi, for all antenna elements, a reference distance of 1 m, and a carrier frequency measured in GHz, and using (2), the path loss can be expressed as

$$\mathrm{PL}_i \ [\mathrm{dB}] = 32 + 10\gamma \log_{10}(d_i) + 20 \log_{10}(f_c), \tag{16}$$

where $\gamma = 2.5$ and $\gamma = 2.8$ for the InF and UMa scenarios, respectively.

B. Network Configuration

We consider a cellular network comprising seven BSs, as shown in Fig. 2. The BSs are deployed in a hexagonal grid layout, which is typical for cellular networks [11]. Unless otherwise specified, the MT position is assumed to be uniformly distributed over the coverage region of cell 1. Both the BSs and the MT are equipped with planar phased-array antennas composed of ideal isotropic radiating elements. The total antenna gain is given as

$$G \ [\mathrm{dBi}] = G_e + G_{\mathrm{BF}}, \tag{17}$$

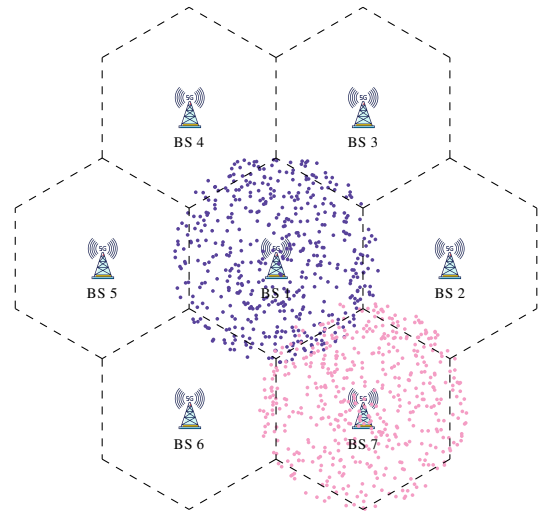

Fig. 2: Cellular layout of a 5G network with seven BSs; the MT is uniformly distributed within the coverage area of the reference cell, i.e., cell 1 and, for comparison, within cell 7.

Parameter	UMa scenario	InF scenario
Network area	$\approx 1,770,000$ m^2	$\approx 18,000$ m^2
Number of involved BSs, N	7	7
Inter-BS distance	500 m	50 m
Carrier frequency, f_c	3.75 GHz	26 GHz
Bandwidth, B	100 MHz	400 MHz
BS transmit power, P_{BS}	30 dBm	24 dBm
BS antenna gain, G_{BS}	6 dBi	12 dBi
MT antenna gain, G_{MT}	6 dBi	12 dBi
BS antenna configuration	2×2	4×4
MT antenna configuration	2×2	4×4
Noise PSD at 293 K, N_0	-174 dBm/Hz	-174 dBm/Hz

TABLE I: 5G network parameters for InF and UMa scenarios.

where G_e is the gain of a single antenna element, and G_{BF} represents the beamforming gain [14]. For an array with N_e antenna elements, the beamforming gain can be expressed as

$$G_{\mathrm{BF}} \ [\mathrm{dB}] = 10 \log_{10}(N_e). \tag{18}$$

Considering thermal noise, the received SNR at the MT from the i-th BS can be calculated as

$$\begin{aligned}\mathrm{SNR}_i \ [\mathrm{dB}] = P_{\mathrm{BS}_i} + G_{\mathrm{BS}_i} + G_{\mathrm{MT}} - \mathrm{PL}_i \\ - (N_0 + 10 \log_{10}(B))\end{aligned} \tag{19}$$

For simplicity, in the simulations of this work, identical correlation behavior is assumed across all BS links, i.e., $\rho_{\tau_i \phi_i} = \rho$, for all i.

The default network parameters are listed in Table I and are used unless we vary a single parameter, in which case all others remain fixed at the values in Table I.

C. Accuracy Metrics

The positioning accuracy is analyzed in terms of the RMSE of the position estimate. For an empirical estimate over N_{mc}

TABLE II: Positioning RMSE in InF and UMa scenarios from Fig. 3.

	Positioning root mean square error (RMSE) (E)			Accuracy Improvement		
	E_{ToA}	$E_{ToA+CP(\rho=0)}$	$E_{ToA+CP(\rho=0.5)}$	$1-\frac{E_{\text{ToA+CP}(\rho=0)}}{E_{\text{ToA}}}$	$1-\frac{E_{\text{ToA+CP}(\rho=0.5)}}{E_{\text{ToA}}}$	$1-\frac{E_{\text{ToA+CP}(\rho=0.5)}}{E_{\text{ToA+CP}(\rho=0)}}$
InF	1.0 cm	0.2 cm	0.1 cm	≈ 84 %	≈ 85 %	≈ 7 %
UMa	24.7 cm	4.0 cm	3.7 cm	≈ 84 %	≈ 85 %	≈ 8 %

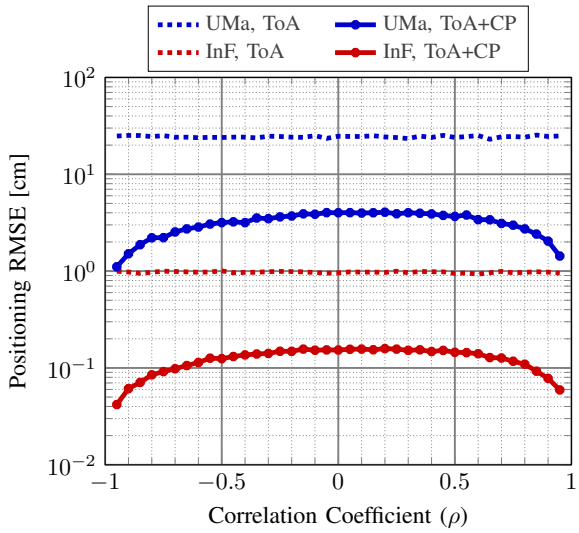

Fig. 3: Positioning RMSE versus correlation coefficient (ρ).

Monte Carlo repetitions, the RMSE of positioning is computed as

$$\text{RMSE} = \sqrt{\frac{1}{N_{\text{mc}}}\sum_{l=1}^{N_{\text{mc}}} \|\mathbf{x}-\hat{\mathbf{x}}_l\|_2^2} \quad [\text{cm}]. \tag{20}$$

IV. Results and Discussion

To show the importance of accounting for the correlation between CP and ToA measurement errors, we assess the impact of the correlation coefficient ρ on positioning accuracy. We then evaluate how key 5G parameters, including bandwidth, carrier frequency, transmit power, antenna configuration, and the number of BSs, influence the positioning accuracy of this method in real 5G networks. Hereafter, the joint correlation-aware positioning method is denoted as *ToA+CP*.

A. Impact of the Correlation Coefficient

Fig. 3 presents the positioning RMSE as a function of the correlation coefficient ρ in the UMa and InF scenarios. As a reference, the RMSE of the conventional ToA method is also included as a horizontal line, since its performance is independent of ρ. The accuracy of the joint ToA+CP method depends strongly on ρ. The results show that the joint ToA+CP method outperforms the conventional ToA method in both UMa and InF scenarios and that its RMSE decreases as $|\rho|$ increases.

This improvement arises because the joint covariance matrix captures the statistical dependence between ToA and CP measurement errors, which can be exploited by the maximum-likelihood estimator. From an estimation-theoretic perspective, correlation modifies the information content of the joint observations; in the considered setup, larger values of $|\rho|$ lead to a lower positioning RMSE. A slight asymmetry between positive and negative values of ρ is also observed, which is attributed to the interaction between the sign of the cross-covariance terms and the nonlinear relationship between the CP and ToA range measurements and the position estimate.

The performance gap between the InF and UMa scenarios is mainly caused by differences in their configuration parameters, as summarized in Table I, such as bandwidth, inter-BS distance, and antenna configuration. This remains true for the following results as well.

Considering a moderate correlation value of $\rho = 0.5$, which may be expected in practice, Table II outlines the positioning errors and corresponding accuracy gains.

B. Impact of Bandwidth

Fig. 4a illustrates the impact of bandwidth on positioning accuracy for both UMa and InF scenarios. The results show, as indicated also in (7), that increasing the bandwidth significantly improves positioning accuracy for both conventional ToA and joint ToA+CP methods. A larger bandwidth enhances the time resolution of the ToA measurements, enabling more precise delay estimation. Across the entire bandwidth range, the joint ToA+CP method consistently outperforms the ToA approach. The incorporation of carrier phase measurements further refines the range estimates, resulting in a substantial reduction in RMSE. Furthermore, the results demonstrate that accounting for correlated measurement errors, i.e., $\rho = 0.5$, yields additional accuracy gains compared to the uncorrelated case, i.e., $\rho = 0$, due to the exploitation of mutual information in both measurements. Comparing both environments, positioning errors in the InF scenario are significantly lower than those in the UMa scenario. This improvement is attributed to the shorter inter-BS distance and higher antenna gains in InF, which lead to improved SNR and reduced measurement variance. At higher bandwidths, the joint ToA+CP method achieves centimeter-level accuracy in both InF and UMa scenarios.

C. Impact of Carrier Frequency

Fig. 4b depicts the effect of carrier frequency, varied from 1 to 100 GHz. The results show that, for the setups considered, positioning accuracy degrades as the carrier frequency increases. This degradation is primarily due to increased path loss at higher frequencies, as indicated in (16), which reduces SNR and increases ToA estimation variance. For the joint

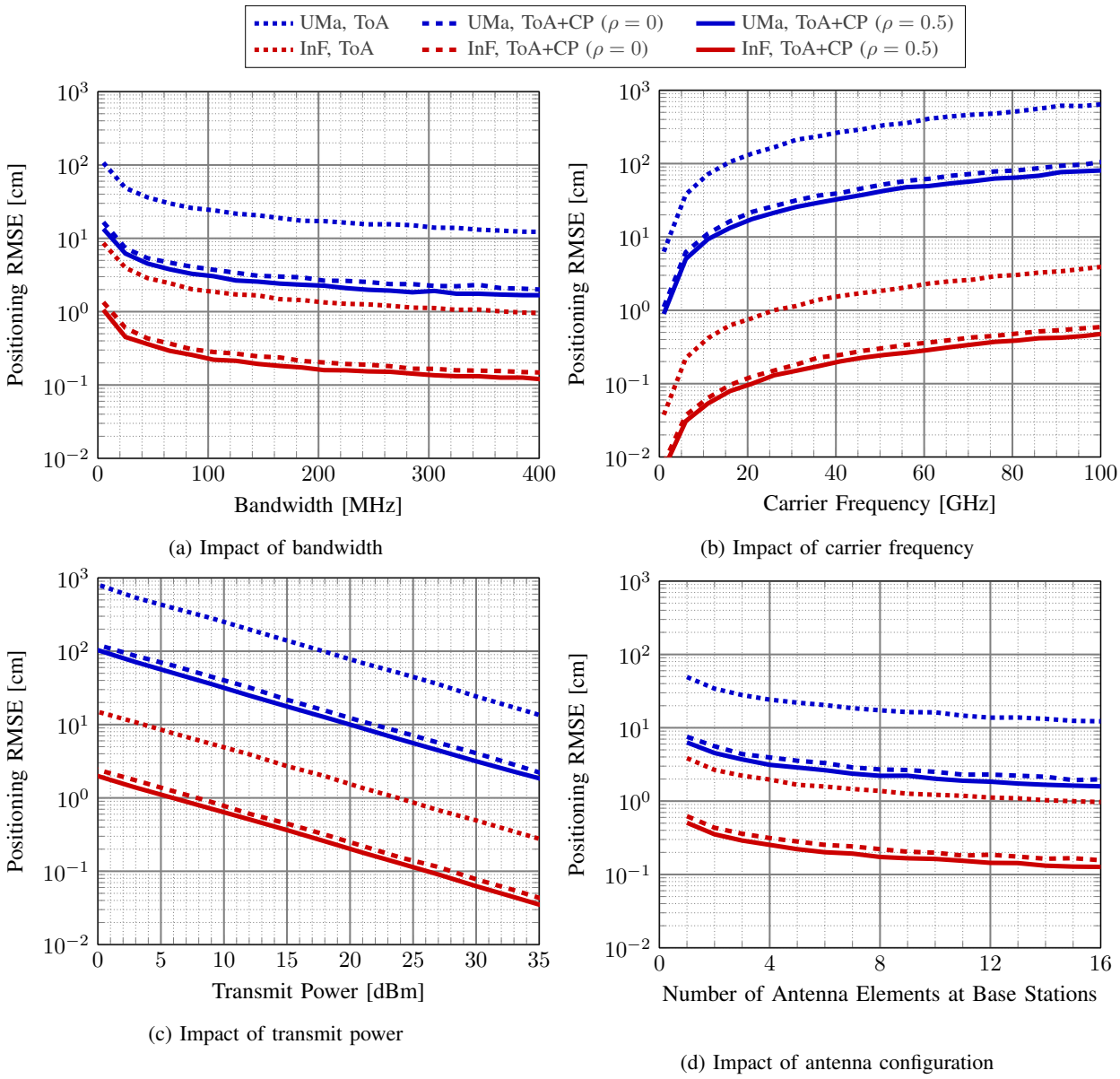

(a) Impact of bandwidth

(b) Impact of carrier frequency

(c) Impact of transmit power

(d) Impact of antenna configuration

Fig. 4: Impact of 5G system parameters on positioning accuracy.

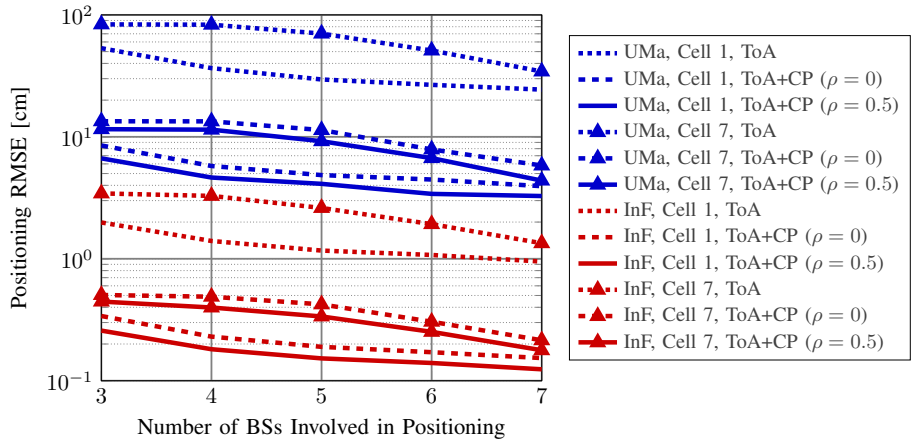

Fig. 5: Positioning RMSE versus the number of participating BSs for two geometries (cell 1 and cell 7).

positioning method, i.e., ToA+CP, the accuracy degradation is less pronounced. Although a higher carrier frequency increases path loss and thus reduces SNR, it simultaneously shortens the carrier wavelength, which improves phase-based ranging precision according to (7). These opposing effects partially compensate for each other, which makes the joint positioning method less sensitive to the carrier-frequency increase than the ToA method.

D. Impact of Transmit Power

Fig. 4c presents the positioning error as a function of transmit power. The results indicate a monotonic reduction in positioning error with increasing transmit power for all methods. Higher transmit power directly increases the received SNR, which reduces both ToA and CP measurement errors according to (7) and thereby lowers the positioning RMSE. As in all other cases, the results show that accounting for correlated measurement errors, i.e., $\rho = 0.5$, yields additional accuracy gains compared to the uncorrelated case, i.e., $\rho = 0$.

E. Impact of Antenna Configuration

Fig. 4d shows the influence of the number of antenna elements in the phased array of BSs, varying from 1 to 16. Increasing the number of antenna elements improves positioning accuracy in both scenarios. This improvement is attributed to the beamforming gain described in (18), which enhances transmit directivity and thereby increases the SNR at the MT. The improved SNR reduces measurement variances for both ToA and CP, leading to lower positioning RMSE. The results demonstrate that antenna array design plays a crucial role in enabling high-accuracy positioning, especially in high-frequency deployments where path loss is severe.

F. Impact of the Number of BSs Involved in Positioning

Figure 5 shows how positioning accuracy is influenced by (i) the number of BSs included in the estimation, which are added sequentially according to their indices, and (ii) the deployment geometry. Two MT locations are considered: (a) a user uniformly distributed within cell 1, representing a geometrically favorable configuration, and (b) a user uniformly distributed within cell 7, representing a less favorable geometry. The results indicate that positioning accuracy generally improves as more BSs are incorporated. This improvement is attributed to enhanced geometric diversity and measurement redundancy. However, the magnitude of this improvement depends strongly on the MT location. When the MT is in cell 1, the surrounding BSs form a favorable spatial configuration; therefore, a substantial reduction in positioning error is achieved with only a few BSs, and adding further BSs yields diminishing returns. In contrast, when the MT is in cell 7, the initial geometry is less favorable, and incorporating additional BSs continues to provide noticeable improvements in accuracy.

V. Conclusions

In this paper, we propose and study a joint positioning method based on ToA and CP measurements in 5G networks, explicitly accounting for the correlation between their measurement errors, as both are extracted from the same received signal and may therefore exhibit correlated errors. The accuracy of the proposed joint positioning method was evaluated as a function of key network parameters using path-loss parameters for the 3GPP-standardized InF and UMa environments. The joint ToA+CP positioning method consistently outperformed the conventional ToA approach. Moreover, the results show that explicitly accounting for measurement-error correlation yields additional positioning accuracy gains in both deployment scenarios. The simulation results further indicate that, under favorable geometry and high-SNR conditions, 5G positioning can achieve centimeter-level accuracy. For future research, we suggest conducting empirical studies to determine the magnitude and distribution of the correlation coefficient between ToA and CP measurements, ρ, in practical implementations.

References

[1] H. Wymeersch, R. Amiri, and G. Seco-Granados, "Fundamental performance bounds for carrier phase positioning in cellular networks," in *GLOBECOM 2023 - 2023 IEEE Global Communications Conference*, 2023, pp. 7478–7483.

[2] Y. Wang, C. Li, H. Wang, and P. Zhu, "Applying carrier phase to 5G positioning with testbed verification," in *2023 13th International Conference on Indoor Positioning and Indoor Navigation (IPIN)*, 2023.

[3] R. Keating, A. Ghosh, B. Velgaard, D. Michalopoulos, and M. Säily, "The evolution of 5G new radio positioning technologies," *Tech. Rep.*, 2021.

[4] 3GPP, "Study on expanded and improved nr positioning enhancements (Release 18)," 3rd Generation Partnership Project, Technical Report 3GPP TR 38.859, June 2024.

[5] S. Fan, Y. Ji, and H. Tian, "Triple-frequency carrier phase positioning with optimized ambiguity resolution in 5g new radio networks," in *GLOBECOM 2023 - 2023 IEEE Global Communications Conference*, 2023, pp. 1191–1196.

[6] J. Nikonowicz, A. Mahmood, M. I. Ashraf, E. Björnson, and M. Gidlund, "Indoor positioning in 5g-advanced: Challenges and solution toward centimeter-level accuracy with carrier phase enhancements," *IEEE Wireless Communications*, vol. 31, no. 4, pp. 268–275, 2024.

[7] P. Teunissen, P. De Jonge, and C. Tiberius, "The least-squares ambiguity decorrelation adjustment: its performance on short gps baselines and short observation spans," *Journal of geodesy*, vol. 71, no. 10, 1997.

[8] K. Pahlavan, *Indoor Geolocation Science and Technology At the Emergence of Smart World and IoT*. River Publishers, 2019.

[9] S. M. Kay, *Fundamentals of statistical signal processing: estimation theory*. Prentice-Hall, Inc., 1993.

[10] J. Li, M. Liu, S. Shang, X. Gao, and J. Liu, "Carrier phase positioning using 5G NR signals based on ofdm system," in *2022 IEEE 96th Vehicular Technology Conference (VTC2022-Fall)*, 2022, pp. 1–5.

[11] 3GPP, "Study on channel model for frequencies from 0.5 to 100 GHz," 3rd Generation Partnership Project (3GPP), Technical Report TR 38.901, January 2020.

[12] S. Sun, T. S. Rappaport, S. Rangan, T. A. Thomas, A. Ghosh, I. Z. Kovacs, I. Rodriguez, O. Koymen, A. Partyka, and J. Jarvelainen, "Propagation path loss models for 5G urban micro- and macro-cellular scenarios," in *2016 IEEE 83rd Vehicular Technology Conference (VTC Spring)*, 2016, pp. 1–6.

[13] T. S. Rappaport, G. R. MacCartney, M. K. Samimi, and S. Sun, "Wideband millimeter-wave propagation measurements and channel models for future wireless communication system design," *IEEE Transactions on Communications*, vol. 63, no. 9, pp. 3029–3056, 2015.

[14] J. Park, D. Jang, H. Choo, and S. Wang, "Design of a dual-band shared-aperture array antenna composed of array elements with high electromagnetic transparency," *IEEE Access*, vol. 12, pp. 137 533–137 541, 2024.